Title
Multi-Resonant Compensation Control for Terminal Capacitance Reduction in Resonant Switched-Capacitor Converters

ISBN
9781665436359

Authors
Zhu, Yicheng
Ye, Zichao
Ge, Ting
et al.

Publication Date
2021-11-05

DOI
10.1109/compel52922.2021.9646068

Proceedings of the 22nd IEEE Workshop on Control and Modeling for Power Electronics (COMPEL 2021), Virtual Conference, Bogotá, Colombia, November 2-5, 2021

Multi-Resonant Compensation Control for Terminal Capacitance Reduction in Resonant Switched-Capacitor Converters

Y. Zhu
Z. Ye
T. Ge
R. C. N. Pilawa-Podgurski

Multi-Resonant Compensation Control for Terminal Capacitance Reduction in Resonant Switched-Capacitor Converters

Yicheng Zhu, Zichao Ye, Ting Ge, and Robert C. N. Pilawa-Podgurski
Department of Electrical Engineering and Computer Sciences
University of California, Berkeley
Email: {yczhu, yezichao, gting, pilawa}@berkeley.edu

***Abstract*—In resonant switched-capacitor (ReSC) converters with the conventional two-phase control, input and output capacitors ($C_{\rm in}$ and $C_{\rm out}$) need to be sufficiently large to ensure ideal input and output behaviors. However, the bulky terminal capacitors dramatically increase the overall converter volume and significantly limit the potential of ReSC converters for achieving higher power density. This paper proposes a multi-resonant compensation control (MRCC) technique for ReSC converters that can adaptively compensate for the negative effects of finite terminal capacitances by ensuring multi-resonant and full zero current switching (ZCS) operation with adjusted duty ratio and switching frequency. The proposed technique is verified experimentally in a 2-to-1 ReSC converter prototype, demonstrating a more than 5 times terminal capacitance reduction without harming the overall efficiency compared to the conventional control technique.**

I. Introduction

Stemming from the conventional pure switched-capacitor (SC) converters [1], [2], resonant switched-capacitor (ReSC) converters utilize high-energy-density capacitors to perform voltage conversion and can achieve both soft-charging and soft-switching operation by the augmenting inductor(s), enabling higher power density and higher efficiency compared to conventional pure SC and magnetics-based converters [3]–[5].

As illustrated in Fig. 1, practical ReSC converters require sufficiently large input and output capacitors (typically $C_{\rm in}$, $C_{\rm out} \geqslant 10C_{\rm fly}$) to stabilize the terminal voltages and ensure ideal input and output behaviors. In practice, such bulky terminal capacitors can be even physically larger than the primary passive components in ReSC converters, which significantly limits the potential of the ReSC topology for higher power density and becomes the bottleneck for converter miniaturization in practice.

Although it is desirable to reduce the size of terminal capacitors in ReSC converters, insufficient terminal capacitances will incur DC bias and asymmetry in the inductor current ($i_{\rm L}$) if the conventional two-phase control with a fixed duty ratio is used, which not only leads to higher output impedance but also prohibits zero current switching (ZCS), resulting in both higher conduction loss and higher switching loss. Since pre-existing models [6]–[8] and analyses [4], [9], [10] of ReSC converters all assume ideal input and/or output behaviors and thus cannot be used to characterize the effects of finite terminal capacitances, [11] proposes a general method for modeling and analyzing ReSC converters with finite terminal capacitances.

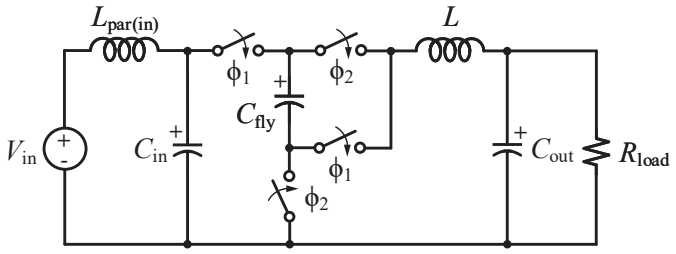

Fig. 1: Schematic of a 2-to-1 ReSC converter with practical input and output. ($L_{\rm par(in)}$: parasitic source inductance)

To adaptively compensate for the negative effects of insufficient terminal capacitances on the performance of ReSC converters, this paper proposes a multi-resonant compensation control (MRCC) technique that can maintain low output impedance and full ZCS capability even when the terminal capacitors are extremely small. In the proposed MRCC technique, the duty ratio and switching frequency are adjusted to ensure multi-resonant operation. With the effects of finite terminal capacitances analyzed in Section II, Section III explains the basic ideas and operating principles of the proposed MRCC technique. In Section IV, the proposed control technique is verified experimentally in a 2-to-1 ReSC converter prototype, demonstrating a more than 5 times terminal capacitance reduction without harming the overall efficiency compared to the conventional control technique.

II. Effect of Finite Terminal Capacitances

According to [11], in a general circuit state (or phase) k, a ReSC converter with finite terminal capacitances can be modeled as the second-order circuit illustrated in Fig. 2. Note that this general expression is applicable to any arbitrary ReSC topologies with a single inductor at output that can achieve full soft-charging operation as long as suitable (topology-dependent) R_k and C_k values are used. For example, for the 2-to-1 ReSC converter shown in Fig. 1, $R_k = 2R_{\rm ds(on)}$ and $C_k = C_{\rm fly}$. As illustrated in Fig. 2, with nonideal input, two

978-1-6654-3635-9/21/$31.00 ©2021 IEEE

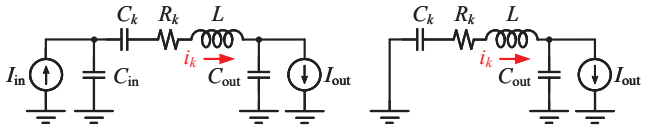

Fig. 2: Second-order circuit model of a two-phase ReSC converter with finite terminal capacitances. (a) Case 1 (Phase 1): the input terminal is connected to the source. (b) Case 2 (Phase 2): the input terminal is grounded. [11]

cases should be considered according to whether the input terminal is connected to the source or ground.

Based on the second-order circuit model provided in Fig. 2, the inductor current in phase k can be expressed as

$$i_k(t) = A_k e^{-\alpha_k t}\cos(\omega_k t + \varphi_k) + I_{fk} \tag{1}$$

where I_{0k} and I_{fk} are the initial value and forced component of i_k in phase k, and τ_k represents the time constant of the equivalent circuit. τ_k and I_{fk} can be expressed as

$$\begin{aligned} \alpha_k &= \frac{R_k}{2L} \qquad \omega_{0k} = \frac{1}{\sqrt{LC_{k(\text{eff})}}} \\ \omega_k &= \sqrt{\omega_{0k}^2 - \alpha_k^2} \qquad I_{fk} = p_k I_{out} \end{aligned} \tag{2}$$

in which α_k, ω_{0k} and ω_k are the decay rate, natural angular frequency and angular frequency of the inductor current in phase k, respectively. $C_{k(\text{eff})}$ is the effective capacitance and p_k is a dimensionless ratio. In the two cases illustrated in Fig. 2, for an m-to-n ReSC converter, $C_{k(\text{eff})}$ and p_k can be given as

$$\begin{aligned} &\text{Case 1 :}\\ &\text{(Phase 1)} \end{aligned} \begin{cases} C_{k(\text{eff})} = 1 \Big/ \left(\dfrac{1}{C_k} + \dfrac{1}{C_{in}} + \dfrac{1}{C_{out}}\right) \\ p_k = \dfrac{C_{k(\text{eff})}}{C_{in}C_{out}}\left(C_{in} + \dfrac{n}{m}C_{out}\right) \end{cases}$$

$$\begin{aligned} &\text{Case 2 :}\\ &\text{(Phase 2)} \end{aligned} \begin{cases} C_{k(\text{eff})} = 1 \Big/ \left(\dfrac{1}{C_k} + \dfrac{1}{C_{out}}\right) \\ p_k = \dfrac{C_{k(\text{eff})}}{C_{out}} \end{cases} . \tag{3}$$

With the above circuit model derived, we can now analyze the effects of finite terminal capacitances. First, from (1)-(3), we can see that insufficient C_{in} and C_{out} will incur DC bias in the inductor current, since I_{fk} will be nonzero when C_{in} and C_{out} are comparable to C_k. Second, (3) indicates that the effective capacitance $C_{k(\text{eff})}$ will be different in the two phases if C_{in} is not sufficiently large. This means that the angular frequency ω_k of the inductor current in the two phases will no long be the same, resulting in asymmetric inductor current waveform. In summary, both insufficient C_{in} and C_{out} can incur DC bias in the inductor current while low C_{in} will further induce an asymmetric inductor current waveform, which will lead to higher RMS inductor current and thus higher output impedance.

Fig. 3 shows the simulated output impedance curves and inductor current waveforms in a 2-to-1 ReSC converter with various terminal capacitances (C_{fly} = 10 μF, L = 0.1 μH, $R_{ds(on)}$ =10 mΩ). Here, we define the intrinsic critical frequency of the 2-to-1 ReSC converter as $f_{crit(int)} = \frac{1}{2\pi\sqrt{LC_{fly}}}$ = 159 kHz. It can be seen in Fig. 3(a) that if we reduce C_{in} or C_{out} to C_{fly} and still operate the converter at $f_{crit(int)}$, the output impedance will significantly rise due to the insufficiency in terminal capacitances. Meanwhile, the influence of C_{in} is quantitatively much stronger than C_{out}, since C_{in} will incur not only DC bias but also asymmetry in the inductor current which can be clearly seen in Fig. 3(b).

To facilitate analysis, we define the critical frequency f_{crit} as the switching frequency at which the minimal value of the inductor current i_L is 0 A. The parameter f_{crit} is typically around the knee of the output impedance curve near the fast switching limit (FSL) impedance and thus usually chosen as the operating point of the converter. Note that f_{crit} differs from $f_{crit(int)}$ since the former can reflect the influence of C_{in} and C_{out} while the latter is independent from the terminal capacitances and determined by only the primary passive components.

Under the conventional control, the output impedance of the 2-to-1 ReSC converter can be reduced by increasing the switching frequency. As shown in Fig. 4(a), we can maintain low output impedance when $C_{in} = C_{fly}$ by increasing the switching frequency from $f_{crit(int)} = 159$ kHz to $f_{crit} = 390$ kHz. However, as can be seen in the time-domain plot of Fig. 4(b), the inductor current waveform at $D = 0.5$ and $f_{crit} = 390$ kHz is no longer half-wave resonant but nearly triangular, prohibiting ZCS at the transition from phase 2 to phase 1. This will result in greatly higher switching loss, especially since the converter now operates at even higher switching frequency, indicating that the terminal capacitances cannot be reduced without harming the overall efficiency when the conventional 0.5-duty-ratio control is used.

III. Multi-Resonant Compensation Control

To reduce the terminal capacitances without sacrificing efficiency, this section proposes a multi-resonant compensation control (MRCC) technique. As explained in Section II, insufficient terminal capacitances will incur DC bias and asymmetry in the inductor current when the conventional control is used. To maintain low output impedance and full ZCS capability when the terminal capacitors are small, the duty ratio should be adjusted to ensure a multi-resonant inductor current waveform as shown in Fig. 4(c). Since the effective capacitance in phase 1 is lower than that in phase 2 (i.e. $C_{1(\text{eff})} < C_{2(\text{eff})}$), the angular frequency of the inductor current is higher in phase 1 (i.e. $\omega_1 > \omega_2$). Since ReSC converters are typically designed to be highly underdamped ($\frac{R}{2}\sqrt{\frac{C}{L}} \ll 1$) [4], the decay rate α_k in (2) is usually much smaller than ω_{0k}, which implies $\omega_k \approx \omega_{0k}$. This means that if we let the inductor current start to oscillate from zero at the beginning of a phase, it will take longer time in phase 2 than in phase 1 for the inductor current to oscillate back to zero again. Therefore, the duty

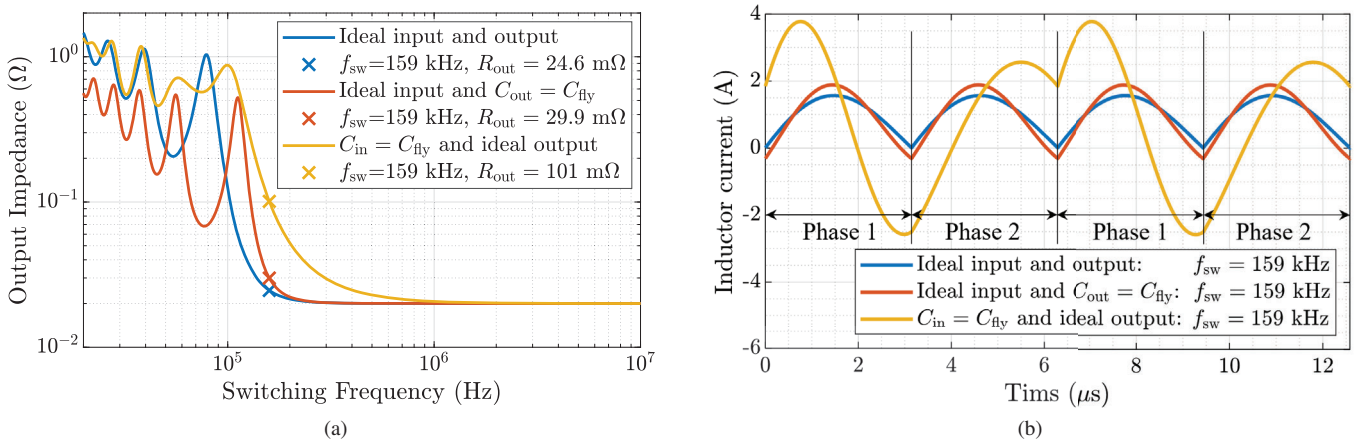

Fig. 3: Effect of terminal capacitances on output impedance and inductor current waveform in the 2-to-1 ReSC converter at the intrinsic critical frequency $f_{\text{crit(int)}} = \frac{1}{2\pi\sqrt{LC_{\text{fly}}}} = 159$ kHz and $D = 0.5$. ($C_{\text{fly}} = 10$ μF, $L = 0.1$ μH, $R_{\text{ds(on)}}$ =10 mΩ) (a) Comparison of output impedance. (b) Comparison of inductor current waveform.

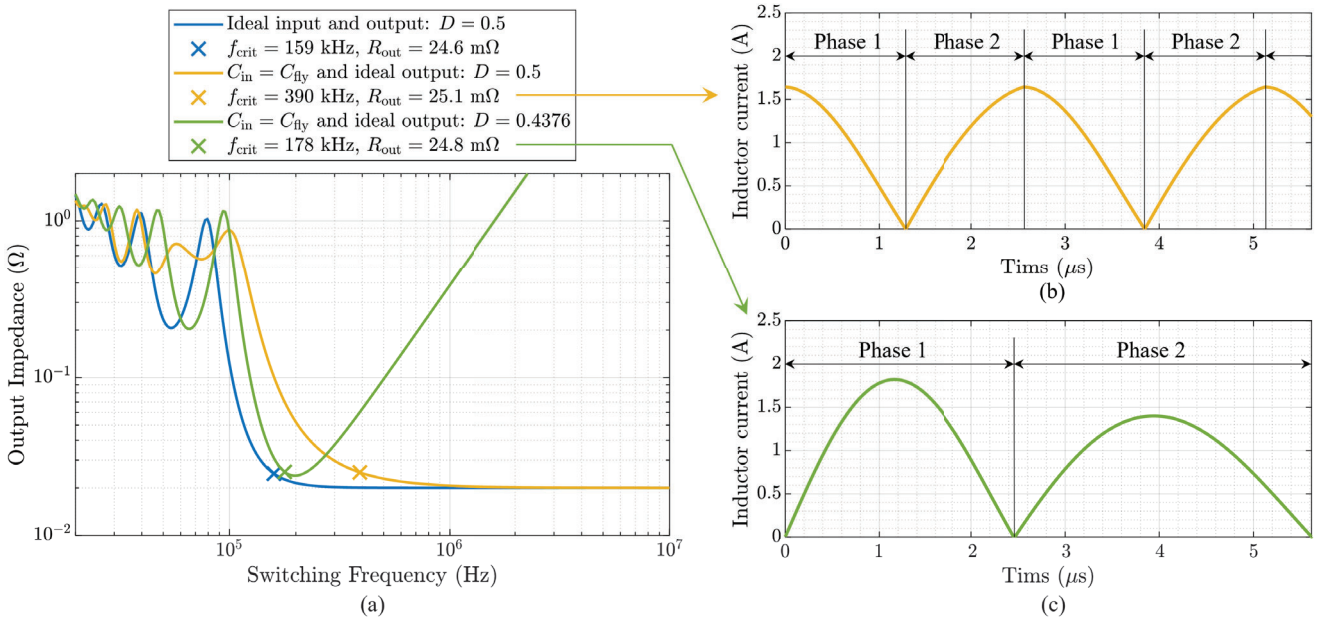

Fig. 4: Comparison between the conventional two-phase control with a duty ratio of 0.5 and the proposed MRCC with the optimum duty ratio and switching frequency. ($C_{\text{fly}} = 10$ μF, $L = 0.1$ μH, $R_{\text{ds(on)}}$ =10 mΩ) (a) Comparison of output impedance. (b) Inductor current waveform of the conventional control ($D = 0.5$ and $f_{\text{crit}} = 390$ kHz). (c) Inductor current waveform of MRCC ($D = 0.4376$ and $f_{\text{crit}} = 178$ kHz).

ratio of phase 1 D_1 should be decreased from 0.5 and the duty ratio of phase 2 D_2 should be increased from 0.5 (i.e. $D_1 + D_2 = 1$ and $D_1 < D_2$). At the optimum duty ratio and switching frequency, we will be able to achieve the multi-resonant inductor current waveform as illustrated in Fig. 4(c).

Next, we need to calculate this optimum duty ratio and switching frequency that ensures multi-resonant operation. First, to achieve full ZCS, the inductor current i_k should be zero at the starting and ending points of each phase:

$$i_k(0) = i_k(D_k T) = 0 \quad (k = 1,\ 2) \tag{4}$$

in which D_k is the duty ratio of phase k and T is the switching period. Moreover, we know that $D_1 + D_2 = 1$. Second, the charge balance in the flying capacitor(s) should be satisfied, which implies

$$\int_0^{D_k T} i_k(t) = a_k I_{\text{out}} T \quad (k = 1,\ 2) \tag{5}$$

in which I_{out} is the output current and a_k is the ratio of the transferred charge in phase k to the total delivered charge in a switching cycle. The definition and calculation of a_k can be found in [2].

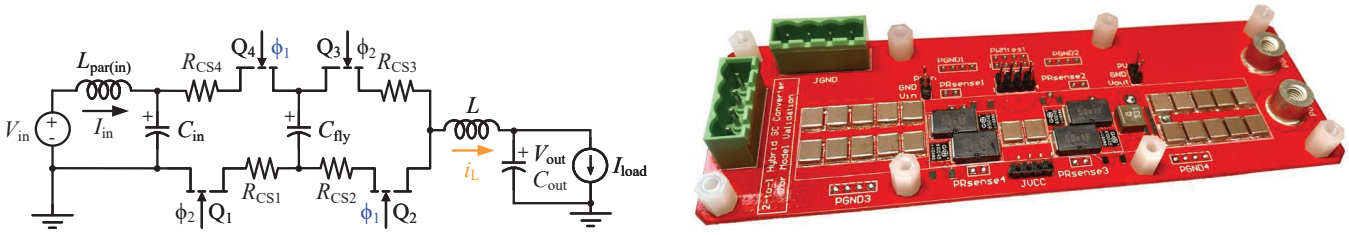

Fig. 5: 2-to-1 ReSC converter prototype. (a) Schematic drawing of the prototype. (b) Photograph of the prototype.

TABLE I: Component List of the 2-to-1 ReSC converter prototype

Component	Part number	Parameters
GaN HEMT Q_1-Q_4	GaN Systems GS61004B	100 V, 16 mΩ (@ 25 °C)
Current sense resistor R_{CS1}-R_{CS4}	KOA Speer SLN5TTED50L0F	50 mΩ, 7 W, 75 PPM/°C
Flying capacitor C_{fly}	KEMET C2220C474J5GACTU	C0G, 50 V, 0.47 μF ×8
Input and output capacitors C_{in} and C_{out}	KEMET C2220C474J5GACTU	C0G, 50 V, 0.47 μF ×8, ×40
Resonant inductor L	Coilcraft XAL6030-331MEC	330 nH, 2.3 mΩ, 30 A
Gate driver	Analog Devices LTC4440-5	80 V, high-side
LDO voltage regulator	Texas Instruments LP2985AIM5-6.1/NOPB	2.5-16 V input, 6.1 V output
Bootstrap diode	Infineon BAT6402VH6327XTSA1	40 V, Schottky diode

Based on (2)-(5), we find that the optimum duty ratio and switching frequency for MRCC is the solution to the following set of equations:

$$\frac{\cosh\left(\alpha_k D_k T\right)-\cos\left(\omega_k D_k T\right)}{\sin\left(\omega_k D_k T\right)}=\frac{\omega_{0k}^2}{2\omega_k}\left(D_k T-\frac{T}{2p_k}\right) \quad (k=1,\ 2). \tag{6}$$

Since $D_1 + D_2 = 1$, there are two unknowns in (6): the duty ratio D_1 (which is defined as the duty ratio of the converter D) and the switching period T (the reciprocal of the switching frequency f_{sw}). Although (6) is a set of transcendental equations that does not have a closed-form analytical solution, it can be conveniently solved with the nonlinear system solver *fsolve* in MATLAB.

IV. Experimental Verification

In this section, a 2-to-1 ReSC converter prototype is specially designed to verify the proposed MRCC technique.

A. Experimental Setup

Figs. 5(a) and (b) show the schematic drawing and photograph of the 2-to-1 SC converter prototype, with main components listed in Table I. The key circuit parameters of the prototype include the flying capacitance $C_{fly} = 3.76$ μF, effective output inductance $L = 388.9$ nH (including parasitic inductance), GaN HEMT on-state resistance $R_{ds(on)} = 16$ mΩ, and current sense resistance $R_{CS} = 50$ mΩ.

As can be seen in 6, the parameters α_k and ω_k are required to calculate the optimum duty ratio and switching frequency, meaning that the equivalent parameters R_k and C_k in Fig. 2 need to be accurately obtained. However, the $R_{ds(on)}$ of GaN HEMTs is prone to large variation under different operating conditions (e.g. junction temperature, drain-to-source current, gate-to-source voltage, etc.) and can be hard to capture due to the dynamic $R_{ds(on)}$ phenomenon [12]. Therefore, to ensure that we can accurately obtain the equivalent resistance R_k, we add a high-precision current sense resistor KOA Speer SLN5TTED50L0F with high thermal stability (75 PPM/°C) in series with each GaN switch to dominate R_k and stabilize it against the variation in $R_{ds(on)}$. In addition, to minimize the variation in capacitances, we choose the Class 1 capacitor KEMET C2220C474J5GACTU which features high capacitance stability over wide range of operating temperature and voltage bias, and extremely low ESR and ESL.

In the experiment, the output impedance is calculated as

$$R_{out}=\frac{V_{in}I_{in}-V_{out}I_{load}}{I_{load}^2}, \tag{7}$$

in which the input voltage V_{in} and input current I_{in} are measured with digital multimeters Keysight 34405A and 34401A, respectively, and the output voltage V_{out} and load current I_{load} are measured by the electronic load Rigol DL3031.

B. Experimental Results

Fig. 6 shows the measured waveforms of MRCC at the optimum D and f_{crit} calculated from (6), in which we can see that MRCC achieves excellent multi-resonant inductor current waveforms and full ZCS even when the input and output capacitors are small. Fig. 7 presents the measured output impedance curves of the 2-to-1 ReSC converter with various C_{in} and C_{out} under the conventional control and MRCC, with

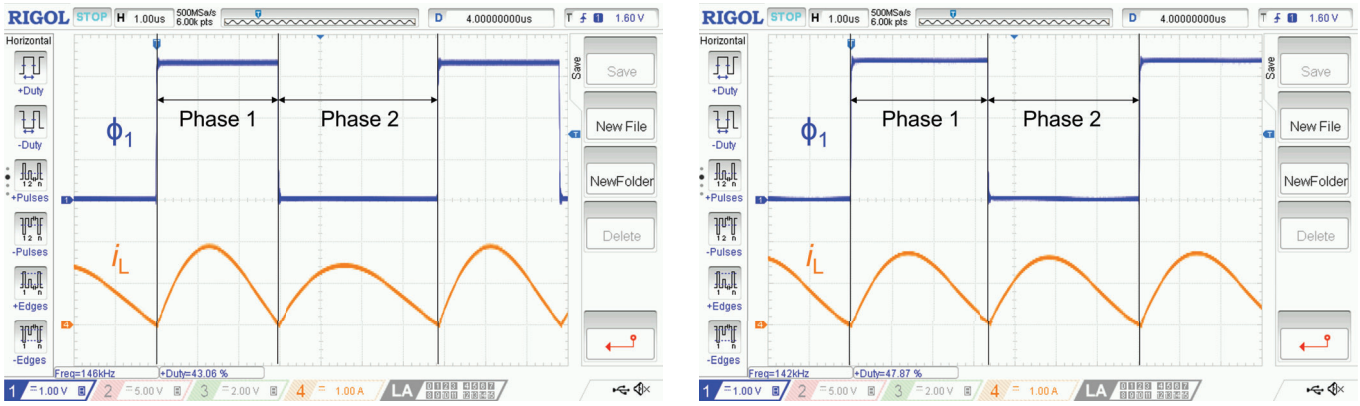

(a) (b)

Fig. 6: Measured waveforms of MRCC at the optimum duty ratio and switching frequency. (ϕ_1: control signal of Q_2 and Q_4, i_L: inductor current) (a) $C_{in} = C_{fly}$, $C_{out} = 5C_{fly}$, $D = 0.4322$, $f_{crit} = 146$ kHz. (b) $C_{in} = 5C_{fly}$, $C_{out} = C_{fly}$, $D = 0.4795$, $f_{crit} = 142$ kHz.

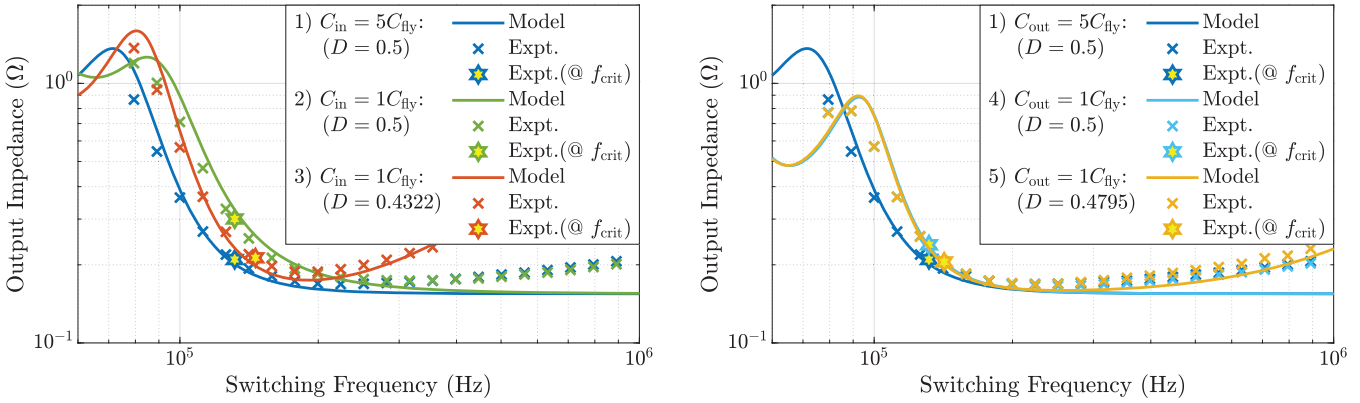

(a) (b)

Fig. 7: Measured output impedance curves with the conventional control and MRCC. (a) Output impedances with various C_{in}. ($C_{out} = 5C_{fly}$) (b) Output impedances with various C_{out}. ($C_{in} = 5C_{fly}$)

the key performance at the critical frequency summarized in Table II.

In Table II, we can see that under the conventional control, the reduction in C_{in} and C_{out} will result in a dramatic increase in output impedance at the critical frequency, meaning that it is impossible to shrink the size of terminal capacitors without harming the overall efficiency. By contrast, MRCC is able to maintain low output impedance even when the terminal capacitors are small, which verifies its capability of reducing the terminal capacitances without harming the overall efficiency.

V. Conclusions

In ReSC converters with the conventional two-phase control, the terminal capacitors need to be sufficiently large to ensure ideal input and output behaviors, which dramatically increases the overall physical volume of the converter and significantly limits the potential of ReSC topologies for achieving higher power density. This paper proposes a multi-resonant compensation control (MRCC) technique for ReSC converters that can adaptively compensate for the negative effects of insufficient terminal capacitances. At the optimum duty ratio and switching frequency, MRCC can ensure multi-resonant inductor current and full ZCS capability even with extremely small terminal capacitors. The proposed control technique is implemented in a 2-to-1 ReSC converter prototype for experimental verification. It is shown that the proposed MRCC technique is able to reduce the terminal capacitances by at least a factor of 5 without harming the overall efficiency.

References

[1] M. S. Makowski and D. Maksimovic, "Performance limits of switched-capacitor DC-DC converters," in *Proceedings of PESC '95 - Power Electronics Specialist Conference*, vol. 2, 1995, pp. 1215–1221 vol.2.

[2] M. D. Seeman and S. R. Sanders, "Analysis and Optimization of Switched-Capacitor DC-DC Converters," *IEEE Transactions on Power Electronics*, vol. 23, no. 2, pp. 841–851, March 2008.

TABLE II: Comparison between the conventional control and MRCC at the critical frequency

No.	$\frac{C_{\text{in}}}{C_{\text{fly}}}$	$\frac{C_{\text{out}}}{C_{\text{fly}}}$	Control method	D	$f_{\text{crit}}{}^{*}$ (kHz)	Calculated R_{out} (mΩ)	Measured R_{out} (mΩ)
1)	5	5	Conventional control	0.5	132	201.3	209.5
2)	1	5	Conventional control	0.5	132	326.3	300.3
3)	1	5	MRCC	0.4322	146	198.1	212.8
4)	5	1	Conventional control	0.5	132	235.9	238.7
5)	5	1	MRCC	0.4795	142	201.0	205.1

* The critical frequency of the conventional control is defined as its intrinsic critical frequency $f_{\text{crit(int)}} = \frac{1}{2\pi\sqrt{LC_{\text{fly}}}} = 132$ kHz, while the D and f_{crit} of MRCC is calculated with (6).

[3] R. C. Pilawa-Podgurski, D. M. Giuliano, and D. J. Perreault, "Merged two-stage power converterarchitecture with softcharging switched-capacitor energy transfer," in *2008 IEEE Power Electronics Specialists Conference*, 2008, pp. 4008–4015.

[4] Y. Lei and R. C. N. Pilawa-Podgurski, "A General Method for Analyzing Resonant and Soft-Charging Operation of Switched-Capacitor Converters," *IEEE Transactions on Power Electronics*, vol. 30, no. 10, pp. 5650–5664, 2015.

[5] Z. Ye, S. R. Sanders, and R. C. N. Pilawa-Podgurski, "Modeling and Comparison of Passive Component Volume of Hybrid Resonant Switched-Capacitor Converters," in *2019 20th Workshop on Control and Modeling for Power Electronics (COMPEL)*, 2019, pp. 1–8.

[6] K. Kesarwani and J. T. Stauth, "Resonant and multi-mode operation of flying capacitor multi-level DC-DC converters," in *2015 IEEE 16th Workshop on Control and Modeling for Power Electronics (COMPEL)*, 2015, pp. 1–8.

[7] S. R. Pasternak, M. H. Kiani, J. S. Rentmeister, and J. T. Stauth, "Modeling and Performance Limits of Switched-Capacitor DC–DC Converters Capable of Resonant Operation With a Single Inductor," *IEEE Journal of Emerging and Selected Topics in Power Electronics*, vol. 5, no. 4, pp. 1746–1760, 2017.

[8] C. Schaef, J. Rentmeister, and J. T. Stauth, "Multimode Operation of Resonant and Hybrid Switched-Capacitor Topologies," *IEEE Transactions on Power Electronics*, vol. 33, no. 12, pp. 10 512–10 523, 2018.

[9] J. S. Rentmeister and J. T. Stauth, "Bypass capacitance and voltage ripple considerations for resonant switched capacitor converters," in *2017 IEEE 18th Workshop on Control and Modeling for Power Electronics (COMPEL)*, 2017, pp. 1–8.

[10] Y. Lei, W.-C. Liu, and R. C. N. Pilawa-Podgurski, "An Analytical Method to Evaluate and Design Hybrid Switched-Capacitor and Multilevel Converters," *IEEE Transactions on Power Electronics*, vol. 33, no. 3, pp. 2227–2240, 2018.

[11] Y. Zhu, Z. Ye, and R. C. N. Pilawa-Podgurski, "Modeling and Analysis of Resonant Switched-Capacitor Converters with Finite Terminal Capacitances," in *2021 IEEE 22nd Workshop on Control and Modeling for Power Electronics (COMPEL)*, 2021.

[12] T. Foulkes, T. Modeer, and R. C. N. Pilawa-Podgurski, "Quantifying Dynamic On-State Resistance of GaN HEMTs for Power Converter Design via a Survey of Low and High Voltage Devices," *IEEE Journal of Emerging and Selected Topics in Power Electronics*, to be published. doi:10.1109/JESTPE.2020.3024930.